Enzymatic resistance to the lipopeptide surfactin as identified through imaging mass spectrometry of bacterial competition

B. Christopher Hoefler[a], Karl V. Gorzelnik[a], Jane Y. Yang[b], Nathan Hendricks[b], Pieter C. Dorrestein[b], and Paul D. Straight[a,1]

[a]Department of Biochemistry and Biophysics, Texas A&M University, College Station, TX 77843; and [b]Skaggs School of Pharmacy and Pharmaceutical Sciences, University of California at San Diego, La Jolla, CA 92093

Edited by Richard Losick, Harvard University, Cambridge, MA, and approved June 28, 2012 (received for review April 3, 2012)

Many species of bacteria secrete natural products that inhibit the growth or development of competing species. In turn, competitors may develop or acquire resistance to antagonistic molecules. Few studies have investigated the interplay of these countervailing forces in direct competition between two species. We have used an imaging mass spectrometry (IMS) approach to track metabolites exchanged between *Bacillus subtilis* and *Streptomyces* sp. Mg1 cultured together. Surfactin is a cyclic lipopeptide produced by *B. subtilis* that inhibits the formation of aerial hyphae by streptomycetes. IMS analysis exposed an addition of 18 mass units to surfactin in the agar proximal to *Streptomyces* sp. Mg1 but not other streptomycetes tested. The spatially resolved change in the mass of surfactin indicated hydrolysis of the molecule. We observed that the aerial growth of *Streptomyces* sp. Mg1 was resistant to inhibition by surfactin, which suggests that hydrolysis was a mechanism of resistance. To identify possible enzymes from *Streptomyces* sp. Mg1 with surfactin hydrolase activity, we isolated secreted proteins and identified candidates by mass spectrometry. We purified one candidate enzyme that hydrolyzed surfactin in vitro. We tested the role of this enzyme in surfactin resistance by deleting the corresponding gene from the *S.* Mg1 genome. We observed that aerial growth by the Δ*sfhA* mutant strain was now sensitive to surfactin. Our results identify an enzyme that hydrolyzes surfactin and confers resistance to aerial growth inhibition, which demonstrates the effective use of an IMS approach to track natural product modifications during interspecies competition.

antibiotic resistance | microbial ecology | secondary metabolism | surfactant

Competition among bacterial species involves the exchange of natural product metabolites, including antibiotics, signals, and toxins (1–6). Natural products benefit producing bacteria through signaling and inhibitory functions toward competitor bacteria (7–9). However, many of these metabolites provide a powerful selection for resistance to emerge within bacterial communities. Recent surveys of microbial communities have demonstrated the widespread nature of antibiotic resistance in the microbial world (10–12). The prevalence of antibiotic producing bacteria in the environment accords with the diverse resistance mechanisms that detect and defuse a range of bioactive natural products (reviewed in ref. 13). One of the hallmark forms of antibiotic resistance is the enzymatic degradation or modification of specific xenobiotic metabolites (14). For example, β-lactamases hydrolyze penicillins, which block their cell wall inhibitory activity and consequent lysis of the exposed cells (reviewed in ref. 15). Enzymatic mechanisms of resistance are not limited to antibiotics. Degradative enzymes that impact competitive interactions also include those that degrade metabolites with signaling functions. For instance, quorum-quenching activities, such as homoserine lactonases, degrade the quorum-signaling compounds that regulate cell-density–dependent functions in competing species (16–18). Enzymes that degrade or modify natural products provide protection by blocking the antagonistic and competitive functions. However, beyond antibiotic resistance, relatively little is known about enzymatic transformations of secreted metabolites that occur during competitive interactions between species of bacteria.

This report focuses on an antagonistic function of the natural product surfactin during bacterial competition between two soil organisms and a mechanism of resistance toward surfactin. Surfactin is a cyclic lipodepsipeptide that is secreted by species of *Bacillus* and disrupts the growth and development of other organisms (19–22). The microbial functions described for surfactin encompass its powerful surfactant activity, antibiotic and antiviral activities, and a recently described paracrine signaling function during biofilm development by *B. subtilis* (23–29). In prior studies of competitive interactions between *Streptomyces coelicolor* and *B. subtilis*, surfactin was found to inhibit streptomycete development of aerial hyphae and spores (30, 31). Despite multiple examples of its antagonistic effects, mechanisms of microbial resistance to surfactin have yet to be described. Instability of surfactin in soils has been reported, suggesting degradation by microorganisms in the environment, but mechanisms for the degradation of surfactin are unknown (32).

Surfactin acts primarily on cellular membranes to disrupt membrane integrity (33). The micelle-forming properties of surfactin, which complement the membrane active properties of the molecule, may complicate the identification of a resistance mechanism. The cyclized peptide moiety of surfactin folds into a "horse saddle" structure that contributes to the exceptional surfactant properties and stability of the molecule (34). The surface activity and stability are in part due to incorporation of L- and D-amino acids, which facilitate folding of the peptide to form an amphipathic headgroup. The complete surfactin molecule also includes a hydrophobic acyl chain, which varies in length, with C_{13}, C_{14}, and C_{15} forms predominant (34, 35). Complete surfactin monomers assemble into micelles at a low critical micellar concentration (CMC), enhancing the surfactant properties of the molecules (36). The overall stability of surfactin most likely arises from the combination of the folded peptide structure, the incorporation of D-amino acids, and the self-association of the monomers. Evidence for limited proteolytic susceptibility of surfactin was discovered in an in vitro study of purified V8 endoprotease from *Staphylococcus aureus* (37). Surfactin peptide cleavage was minimal in these experiments, degrading ~14% of the total metabolite pool, despite extensive incubation with the enzyme. Thus, the identity of enzymes that efficiently degrade surfactin remains uncertain.

Here, we report the identification of a mechanism of surfactin resistance from a soil actinomycete, *Streptomyces* sp. Mg1

Author contributions: B.C.H., P.C.D., and P.D.S. designed research; B.C.H., K.V.G., J.Y.Y., and N.H. performed research; B.C.H., K.V.G., P.C.D., and P.D.S. analyzed data; and P.D.S. wrote the paper.

The authors declare no conflict of interest.

This article is a PNAS Direct Submission.

[1]To whom correspondence should be addressed. E-mail: paul_straight@tamu.edu.

This article contains supporting information online at www.pnas.org/lookup/suppl/doi:10.1073/pnas.1205586109/-/DCSupplemental.

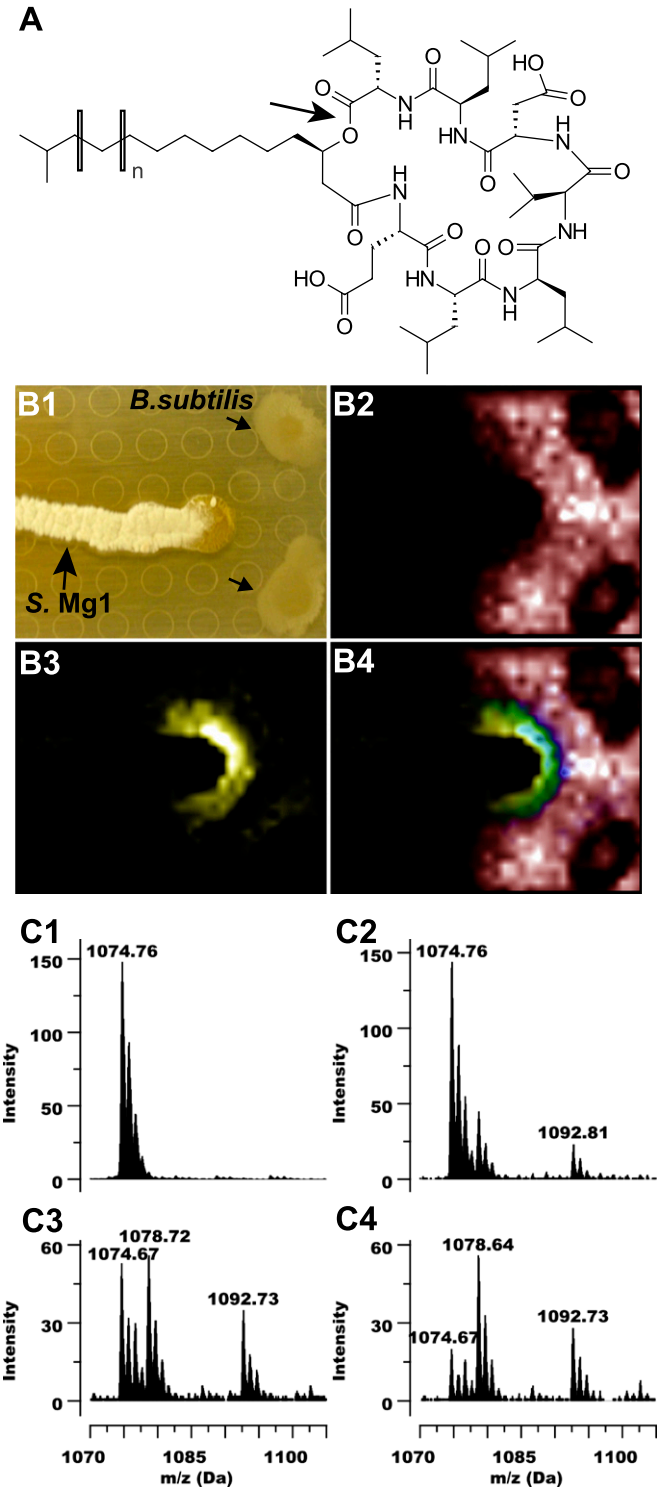

Fig. 1. IMS of surfactin from *B. subtilis* 3610 with *Streptomyces* sp. Mg1. (*A*) The structure of surfactin with the variable length acyl chain indicated in brackets ($(\|_n$), and the bond forming the lactone marked with an arrow. (*B1*) Image of *B. subtilis* and *S.* Mg1 cultured for IMS (*Materials and Methods*). *S.* Mg1 (vertical arrow) was inoculated as a streak of spores. *B. subtilis* (small arrows, right) was inoculated in two spots to the right of *S.* Mg1. The images (*B2–B4*) depict ions for C_{13}-surfactin (*m/z* 1047, red; *B2*) and hydrolyzed (+18 *m/z*) C_{13}-surfactin (*m/z* 1065, yellow; *B3*). An overlay of *B1* and *B2* illustrates the relative spatial distribution of ions (*B4*), revealing surfactin hydrolysis in proximity to the *S.* Mg1. (*C*) Single spectra from the imaging data of a *B. subtilis* 3610 and *S.* Mg1. An increase in surfactin +18 *m/z* ion intensity occurs with a corresponding reduction in the intact surfactin ion intensity. The spectral window is limited to the range *m/z* 1070–1105 to highlight representative C_{15}-surfactin $[M+K]^+$ (*m/z* 1074.76) and hydrolyzed surfactin ions $[M+K+H_2O]^+$ (*m/z* 1092.81) in succession from near the *Bacillus* colony (*C1*), at the midpoint between the colonies (*C2*), and near the *S. Mg1* colony (*C3* and *C4*). Note: *m/z* 1078.72 is the hydrolyzed $[M+K+H_2O]+$ ion of C_{14}-surfactin (*m/z* 1060.75).

(*S.* Mg1), in a competitive interaction with *B. subtilis*. To follow the fates of surfactin and other natural products in competition with *S.* Mg1, a MALDI-TOF–based imaging mass spectrometry (IMS) approach was used (31, 38, 39). IMS provided a method to track in situ the secretion and modification of surfactin during interspecies interactions. The IMS data suggested that *S.* Mg1 hydrolyzes surfactin. Specifically, we observed a spatially localized +18 *m/z* mass change for surfactin as it diffused from colonies of *B. subtilis* toward colonies of competing *S.* Mg1. Several species of *Streptomyces* were tested for sensitivity to surfactin-induced balding. *S.* Mg1 was found to be the only species of those tested that could form aerial hyphae in the presence of surfactin. The detection of surfactin hydrolysis during interspecies competition led to efficient identification and purification of the hydrolyzing enzyme produced by *S.* Mg1. We reasoned that this enzyme could provide a surfactin resistance mechanism for *S.* Mg1, which was confirmed by deletion of the gene encoding the surfactin hydrolase.

Results

Imaging Mass Spectrometry Reveals Surfactin Degradation. In a survey of streptomycetes cultured with *B. subtilis* NCIB3610, we observed that aerial growth and spore development were disrupted to varying degrees for several species of *Streptomyces* (Fig. S1). Based on our previous observation that surfactin inhibits aerial development of *S. coelicolor*, which we describe as a balding effect, we hypothesized a role for surfactin in these competitive interactions (Fig. 1*A*) (30, 31). However, the relative differences in growth, development, and metabolism of the two organisms in coculture obscure the functions of individual metabolites. As an approach to monitoring natural products, including surfactin, during competitive interactions between *B. subtilis* and streptomycetes, we used MALDI-imaging mass spectrometry (IMS) (31, 40). *B. subtilis* and *Streptomyces* spp. are commonly isolated from soils where they compete for resources when they are actively growing. We focused on one species in particular, *Streptomyces* sp. Mg1 (*S.* Mg1), because we isolated the strain in parallel with strains of *B. subtilis* from a single sample of soil in which the species may naturally compete (41).

We used IMS to monitor the production and fate of natural product metabolites in the competitive interaction between *B. subtilis* NCIB3610 and *S.* Mg1 (31, 40). Application of IMS enabled spatial tracking of metabolites in the mass range that we surveyed, 500–3000 *m/z*. For surfactin, multiple ions are detected as a result of its variable-length acyl chain (Fig. 1*A*). Individual surfactin ions are separated by 14 mass units: *m/z* 1047 $[C13 + K]^+$, *m/z* 1061 $[C14 + K]^+$, and *m/z* 1075 $[C15 + K]^+$. This typical pattern of surfactin ions was detected in the space between the *B. subtilis* colonies and *S.* Mg1 (Fig. 1*B2*). Near the *S.* Mg1 colony, new ions could be identified from the spectra in the same mass range as the surfactins. Curiously, we noted that with increasing proximity to *S.* Mg1, the newly visible peaks in the IMS spectra corresponded to each surfactin ion +18 *m/z* (Fig. 1 *B3* and *C*). Progression through the sequence of images of Fig. 1 illustrates the spatial distribution of the new ions. Individual mass spectra from selected positions in the coculture show an increase in intensity of the new ions near *S.* Mg1 (surfactin +18 = *m/z* 1093) concomitant with a decrease in the intensity of the parent surfactin ion (*m/z* 1075). This observed pattern suggests the +18 *m/z* ions are surfactins undergoing hydrolysis by an activity secreted from *S.* Mg1. To confirm the +18 *m/z* ions were related to the surfactin ions, and not unique metabolites secreted by *S.* Mg1, we fragmented the ions by using tandem MS/MS. The resulting patterns of b- and y-ion fragmentation for the +18 *m/z* ions were

consistent with their identity as hydrolyzed C13, C14, and C15 surfactins (Fig. S2). Intriguingly, similar results were obtained from IMS and tandem MS/MS analysis of plipastatin, a second lipopeptide synthesized by *B. subtilis* (Fig. S3). Surfactin and plipastatin peptides are both macrolactones, but they differ in amino acid composition and lipid chain length. The structural differences between the molecules suggest that *S.* Mg1 secretes either a hydrolytic activity that cleaves both surfactin and plipastatin or multiple activities that target the substrates specifically.

Aerial Development of *Streptomyces* sp. Mg1 Is Resistant to Surfactin. Identification of hydrolyzed surfactin near the *S.* Mg1 colony suggested this streptomycete is resistant to surfactin. We tested *S.* Mg1 and other streptomycetes for aerial growth in the presence of the purified compound (Fig. 2). Surfactin spotted on the center of a uniform lawn of bacteria caused areas of balding with diameters of ~1–3 cm, depending on the species. In addition to balding, some of the species tested were growth inhibited at the site of surfactin deposition, in contrast to the diffuse area of surfactin-induced balding. This report focuses solely on the balding effect of surfactin. Direct application of surfactin failed to block aerial development of *S.* Mg1 at concentrations that inhibit aerial hyphae formation in all of the other strains tested (Fig. 2). Based on the results of our imaging and culture assays, we reasoned that the soil isolate *S.* Mg1 secretes an enzyme that provides resistance to surfactin-induced balding through the hydrolysis of surfactin.

Identification of a Putative Surfactin Hydrolase via Analysis of *S.* Mg1 Secreted Proteins. Suspecting an enzymatic mechanism of resistance to surfactin, we predicted the enzyme responsible could be identified from the agar media of a *S.* Mg1 culture plate. Agar was collected from the area surrounding the streptomycete mycelium, and soluble proteins were extracted and concentrated. A collection of secreted proteins was detected by Coomassie staining of an SDS/PAGE gel, and the proteins were identified by tandem LC/MS/MS (Fig. S4*A* and Table S1). Many of the proteins identified were annotated as degradative enzymes, including proteases, lipases, and other hydrolases. When grouped by annotated function, several of the identified proteins were predicted to have hydrolytic activity on peptide or protein substrates (Table 1). Highly similar orthologous sequences could be identified for some candidates by using BLAST searches of available *Streptomyces* spp. genomes. However, a candidate protein that was annotated "secreted hydrolase" (gi|254386602) was notable for its sequence divergence from its closest relatives, including those from nonsurfactin degrading species (Table S2). We cloned this putative secreted hydrolase gene and other candidate genes from *S.* Mg1 for recombinant expression, purification, and in vitro testing.

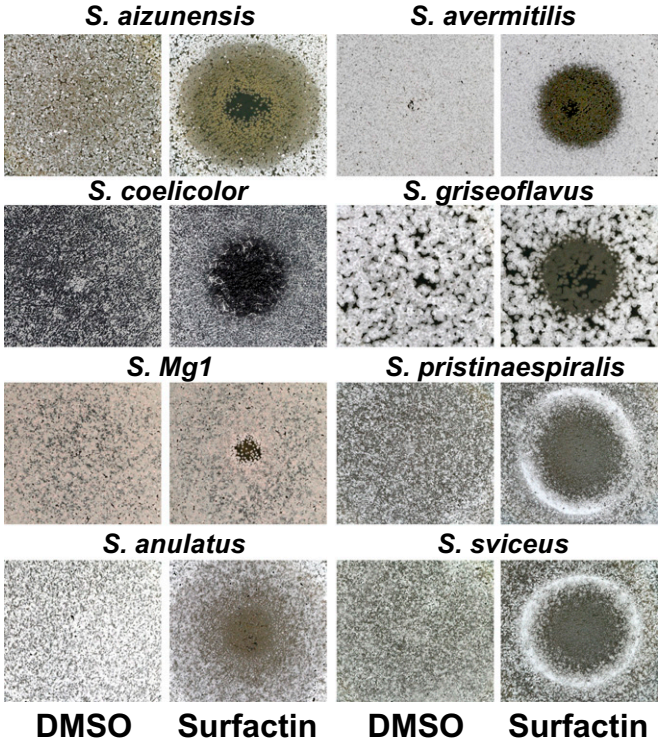

Fig. 2. *S.* Mg1 is resistant to the surfactin induced balding seen with several *Streptomyces* spp. *Streptomyces spp*. were plated on mineral supplemented MYM7 media as uniform density lawns and incubated at 30 °C until aerial development was observed. Spotted in the center of each plate were either DMSO as a control (*Left* and *Left Center*) or purified surfactin dissolved in DMSO to 20 mg/mL (*Right Center* and *Right*). Surfactin sensitivity is seen as a bald patch in the plate center. Only *S.* Mg1 develops aerial hyphae with surfactin. Species are as labeled and listed in Table S3.

Expression and Purification of a Surfactin Hydrolase. A cloned copy of the candidate hydrolase gene was expressed with a 6×-histidine tag in *Escherichia coli*. We detected an ~54-kDa band in whole cell lysates of *E. coli* expressing the secreted hydrolase gene. Assays of the cell lysates by MALDI-MS showed hydrolysis of surfactin (Fig. S4). Because the protein was largely insoluble in *E. coli*, affinity purification was carried out under denaturing conditions on a Ni^{+}-NTA resin. The purified, unfolded protein was gradually refolded by stepwise removal of the denaturant (Fig. S4*B*, lanes C1 and C2). In an in vitro assay, 320 ng of the purified enzyme catalyzed rapid hydrolysis of 50 μM surfactin in a 100-μL reaction over a period of 10–30 min (Fig. 3). Intact surfactin ions (1029, 1043, 1057, 1065, and 1079 $[M + Na]^{+}$) diminished over the course of the reaction, whereas hydrolyzed surfactin +18 *m/z* ions emerged (1047, 1061, 1075, 1083, 1097 $[M + Na]^{+}$). A control reaction without the secreted hydrolase showed no change in the spectrum of surfactin over a 2-h time period (Fig. 3). Based on the in vitro enzyme activity, we conclude that the enzyme functions as a surfactin hydrolase. We considered the possibility that the enzyme could hydrolyze other lipopeptide or macrolactone substrates. To test this possibility, we incubated surfactin hydrolase with several lipopeptides and cyclic antibiotics as well as iturin A, which is cyclized via a lactam instead of lactone (Table 2 and Fig. S5). Surfactin and plipastatin were the only substrates to be cleaved by the surfactin hydrolase in these assays.

Surfactin Hydrolase from *S.* Mg1 Cleaves the Ester That Forms the Macrocycle of Surfactin. Analysis of the tandem mass spectral data used to identify the surfactin +18 *m/z* ions suggested that hydrolysis occurs at the ester of surfactin, but hydrolysis elsewhere in the peptide could not be excluded (Fig. S2). To confirm the site of hydrolysis, we prepared a sample of enzyme-hydrolyzed surfactin and determined the cleavage site by 2D NMR (HSQC). Intact, cyclic surfactin shows a C3 (71.4 ppm)–H3 (5.06 ppm) correlation from the methine (C-H) adjacent to the ester in the acyl chain that is clearly resolved from the other aliphatic resonances (Fig. S6). Consistent with hydrolysis of the ester, this correlation shifts upfield in both dimensions, C3 (67.0 ppm)–H3 (3.70 ppm), for the enzyme-treated surfactin. Together with the tandem MS data for the ions near *S.* Mg1 (Fig. S2), these observations support hydrolytic cleavage of the lactonizing ester, which results in a linear surfactin +18 *m/z* product.

Surfactin Hydrolase Provides a Mechanism of Resistance to Surfactin-Induced Balding of *S.* Mg1. Identification of the secreted hydrolase enabled us to ask whether the enzyme confers resistance to surfactin-induced balding. The gene encoding the surfactin hydrolase (denoted as *sfhA*) was deleted from the *S.* Mg1 genome to obtain the Δ*sfhA* strain (PDS0366). When cultured in isolation, the Δ*sfhA* mutant strain showed no apparent phenotype in growth, sporulation, or pigmentation, which were similar to wild type. However, the Δ*sfhA* strain was unable to hydrolyze

Table 1. Secreted hydrolases from *Streptomyces* Mg1

Protein annotation	NCBI gi identifier	Protein molecular mass, Da
Secreted tripeptidylaminopeptidase	254384290	58089.9
Peptidase S8 and S53 subtilisin kexin sedolisin	254381890	51429.4
Secreted hydrolase	**254386602**	**53901.7**
Serine protease	254382793	114805.7
Trypsinogen	254387105	26540.7
Streptogrisin-B	254387168	29877.1
Phospholipase D	254384004	35716.5
Leupeptin-inactivating enzyme 1	254382420	45319.5

Secreted proteins from the media surrounding an *S.* Mg1 colony were identified by LC/MS/MS. The proteins were grouped by their annotated function. Proteins with predicted hydrolytic activity on peptide or protein-like substrates are shown. The surfactin hydrolase is highlighted in bold.

surfactin as detected by IMS (Fig. 4*A* and Fig. S4). We sought to determine whether the Δ*sfhA* strain is sensitive to surfactin, and whether the linearized surfactin retains inhibitory activity toward aerial development of streptomycetes. Hydrolyzed surfactin was obtained in a reaction with surfactin hydrolase until no cyclized form was detected by MALDI-MS (estimated ≥95% hydrolyzed). To confirm that in vitro hydrolysis disrupted the aerial inhibitory activity, we applied equal amounts of intact and linearized compound to the wild-type strain of *S. avermitilis*, which is highly sensitive to surfactin induced balding. The *S. avermitilis* formed aerial hyphae in the presence of hydrolyzed surfactin but not intact surfactin (Fig. 4*B*). Some residual effects of the hydrolyzed surfactin were observed with this strain, which may reflect a low level of activity from the linear surfactin or may be due to a small amount of cyclic surfactin remaining (estimated ≤5%). Consistent with previous observations, the wild-type *S.* Mg1 showed no balding sensitivity to either the intact surfactin or the enzyme-hydrolyzed surfactin. By contrast, the *S.* Mg1 Δ*sfhA* mutant strain was sensitive to intact surfactin, which was detected as an area of balding on the lawn of sporulating bacteria (Fig. 4*B*). This unprecedented balding of *S.* Mg1 upon treatment with purified surfactin indicates that resistance was abolished by deletion of the enzyme. A cloned copy of the *sfhA* gene complemented the deletion when integrated in single copy into the genome of the mutant strain, confirming the specific function of the hydrolase in resistance to balding (Fig. 4 and Fig. S4). Accordingly, we observed no balding activity upon treatment of any *S.* Mg1 strain with previously hydrolyzed surfactin, indicating that only the cyclic form blocks aerial development.

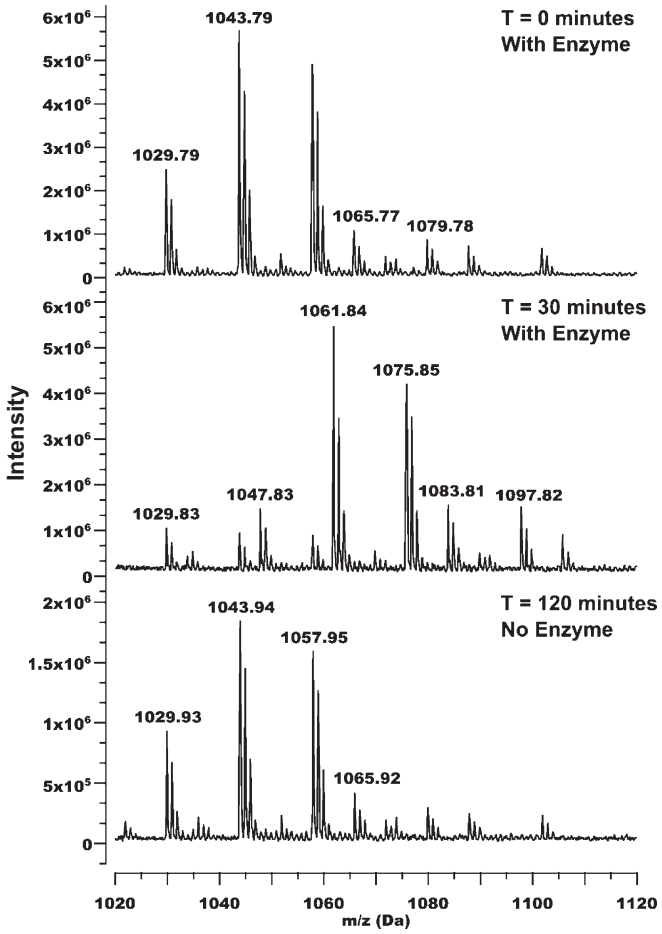

Fig. 3. MALDI-TOF assay reveals surfactin hydrolysis by the purified secreted hydrolase. MALDI-TOF mass spectra of surfactin ions following reaction with the purified secreted hydrolase. The reactions were quenched with acetone at the indicated times. The *m/z* 1020–1120 spectra show results of reactions with enzyme quenched at 0 (*Top*) and 30 min (*Middle*) and without enzyme at 120 min (*Bottom*). After 30 min of incubation with enzyme, the majority of surfactin is hydrolyzed to (surfactin +18 *m/z*).

Discussion

Enzymatic mechanisms of antibiotic resistance have been described as "the apogee of the bacterial antibiotic countermeasures" (13). Enzymes with high specificity for xenobiotic substrates provide resistance to a range of antibiotics and may acquire mutations that expand their substrate range (42). The natural functions of these enzymes are found within microbial communities, which function as reservoirs of antibiotic resistance within diverse environments, including the human microflora and soils (10, 11). Here, we have used an IMS strategy to identify an enzymatic activity that hydrolyzes surfactin, which provides *S.* Mg1 with a mechanism of resistance to the balding effects of the molecule. Surfactin from *B. subtilis* has been investigated extensively for its multiple functions, potential medical and industrial applications, and as a model for natural product enzymology (21, 43, 44). We focused on the antagonistic function of surfactin in blocking development of aerial filaments by streptomycetes. The recognition of surfactin hydrolysis by IMS led to the targeted purification and characterization of the active hydrolase. We found that the surfactin hydrolase secreted by *S.* Mg1 efficiently degrades surfactin from *B. subtilis*. The *sfhA* gene was then deleted from the *S.* Mg1 genome, which resulted in the strain converting from surfactin resistant to surfactin sensitive.

Based on sequence comparisons to known enzymes, the surfactin hydrolase is a secreted enzyme of the tripeptidyl aminopeptidase (TAP) hydrolase family (45). The protein sequence of the surfactin hydrolase contains 499 amino acids with a predicted molecular mass of ~54 kDa. The conserved domains within the protein include an α/β hydrolase_1 folded domain (pfam00561, *E* value 5.84×10^{-6}), characteristic of a wide range of hydrolases from many species. A second domain near the C-terminal end of the protein is of the α/β hydrolase_4 type found in TAP enzymes from *Streptomyces lividans* (pfam08386, *E* value

Table 2. Surfactin hydrolase specificity for surfactin and plipastatin compared with other potential lipopeptide and macrocyclic substrates

Compound	Hydrolysis*
Surfactin	+
Plipastatin	±
Iturin A	–
Daptomycin	–
A54145D	–
Nystatin	–
Amphomycin	–
Amphotericin B	–
Erythromycin	–
CDA[†]	–

The purified hydrolase was incubated with the metabolites listed for 30 min. +, ~95% hydrolysis; ±, some hydrolysis; –, no hydrolysis detected under conditions used.
*See Fig. S5 for corresponding mass spectra.
[†]Calcium-dependent antibiotic.

1.10×10^{-9}) and belongs to the esterase-lipase superfamily based on the conserved catalytic core. Despite the presence of genes encoding similar hydrolases, we did not detect surfactin hydrolysis activity from other *Streptomyces* species tested. The *S.* Mg1 enzyme may have some intriguing structural differences that confer substrate specificity for surfactin but also show diminished hydrolysis of plipastatin and possibly other lipopeptides. Together with our experimental results, the primary sequence information for the enzyme supports its observed function as a lipopeptide hydrolase variant of a larger family of secreted hydrolases.

Surfactin belongs to the lipodepsipeptide class of natural products, which includes antibiotics such as daptomycin and ADEPs (46, 47). Although the surfactin hydrolase had activity against the lipopeptide plipastatin in addition to surfactin, other compounds tested were not substrates for the enzyme. The ability of the enzyme to hydrolyze two structurally different substrates suggests that one or a few random mutations in the surfactin hydrolase gene may produce an enzyme permissive for hydrolysis of daptomycin or other lipopeptides. Studies on enzyme promiscuity toward substrates such as plipastatin and daptomycin, as well as structural characterization of the substrate-binding domain, will be of interest. This report demonstrates that bacterial competition and IMS is a useful tool for discovery of activities that degrade many types of natural products. In particular, the imaging strategy described is a unique method for discovering and understanding antibiotic resistance and could be applied to a range of microbial communities and interactions.

Materials and Methods

Bacterial Strains and Media. The strains used for this study were *B. subtilis* 3610 (PDS0066), *S.* Mg1 wild type (PSK0558), Δ*sfhA* (PDS0366), and Δ*sfhA*, sfhA ApR (PDS0424). Other *B. subtilis* and *Streptomyces* spp. are as listed in *SI Materials and Methods*. Spore suspensions of *Streptomyces* spp. were prepared by using standard procedures (48) and used for the described plating experiments. Bacto media reagents were used unless otherwise indicated. Media for *Streptomyces* growth [Glucose, Yeast-Extract, Malt-Extract (GYM) and Malt-extract Yeast-extract Maltose (MYM)] and coculture conditions are described in *SI Materials and Methods*. Surfactin, amino acids, thiamine-HCl, Mops, and Universal Matrix were purchased from Sigma-Aldrich along with other chemical reagents, unless otherwise noted. All solvents used were HPLC grade. The *E. coli* WM3780 strain was used as the donor strain for conjugation with *S.* Mg1 (49). *E. coli* XL10-Gold and XL1-Blue strains (Stratagene) were used for cloning, and the *E. coli* Rosetta (DE3) strain (Novagen) was used for protein overexpression. For long-term storage, bacterial strains were preserved cryogenically at –80 °C in water (*Streptomyces* spp. spores) or 20% (vol/vol) glycerol (*B. subtilis* and *E. coli*). The primers used in this study are listed in Table S4.

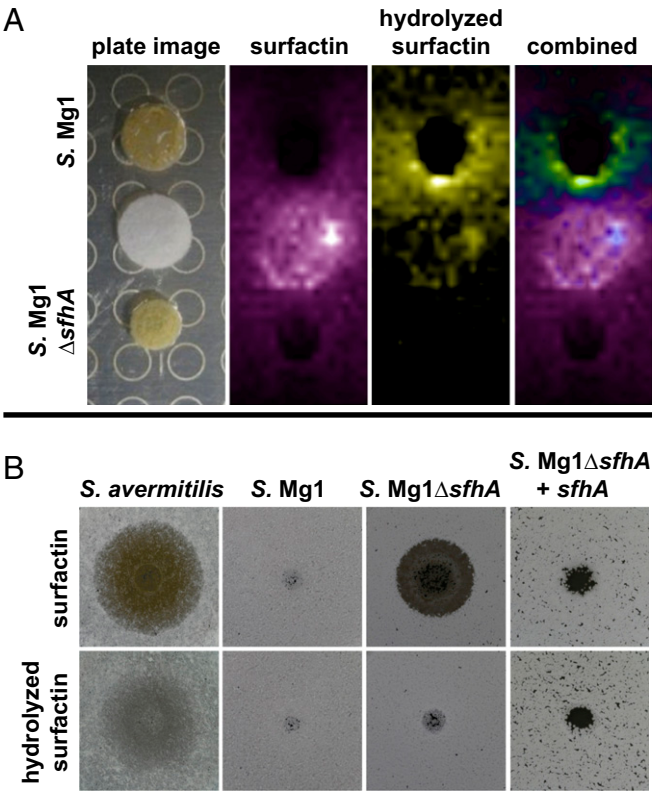

Fig. 4. The Δ*sfhA* mutant strain does not hydrolyze surfactin and is sensitive to surfactin-induced balding. (*A*) Purified surfactin (70 μg) was placed on a filter between the wild-type (*Upper*) and Δ*sfhA* (*Lower*) strains. The IMS depicts hydrolysis of the *m/z* 1074 ion of surfactin (lavender) to the *m/z* 1092 (+18 *m/z*) form (yellow) by the wild-type strain but not the Δ*sfhA* strain. (*B*) Untreated surfactin (*Upper*) or hydrolyzed surfactin (*Lower*) (~100 μg) was applied to lawns of *S. avermitilis*, wild-type *S.* Mg1, the Δ*sfhA*, and the complemented (Δ*sfhA* + *sfhA*) strains. After the onset of aerial development, "bald" patches due to surfactin are on the plates. *S. avermitilis* is highly sensitive to cyclized surfactin but not to enzymatically hydrolyzed surfactin. Wild-type *S.* Mg1 produces aerial hyphae in the presence of both cyclized and hydrolyzed surfactin. Aerial hyphae are blocked by surfactin, which is seen as a bald patch on the Δ*sfhA* mutant strain of *S.* Mg1. The genetically complemented mutant (Δ*sfhA* + *sfhA*) grows aerial hyphae similar to wild type when treated with surfactin. When hydrolyzed by the purified enzyme, surfactin does not block aerial hyphae.

Cultures of *Streptomyces* spp. with *B. subtilis* or Purified Surfactin. Coculture experiments were generally carried out as previously described (30) (*SI Materials and Methods*). The spore density for plating was varied between 10^4 and 10^6 spores per 100-mm plate to obtain consistent and even aerial development across the plate. Buffered GYM was the preferred media for coculture, but supplemented MYM was used for *S. pristinaespiralis*. Mineral supplemented, buffered MYM was used for surfactin tests, except in the case of *S. aizunensis* where supplemented, buffered GYM was used. Purified surfactin was dissolved in DMSO at a concentration of 20 mg/mL. Hydrolyzed surfactin was prepared enzymatically, as described for the NMR analysis (*SI Materials and Methods*), and redissolved after desalting to a concentration of 20 mg/mL in DMSO. Aliquots (5 μL) of surfactin, hydrolyzed surfactin, or DMSO as a negative control were added to the center of each plate. The plates were incubated at 30 °C as described for cocultures until aerial hyphae were observed.

MALDI IMS. The format for coculture of *B. subtilis* with *S.* Mg1 (*SI Materials and Methods*) was altered slightly to be more suitable for the MALDI imaging experiments. A spore suspension was inoculated in a dense format as either a line across the plate, or in evenly spaced 6-μL drops across the plate (Fig. S3). *B. subtilis* was inoculated (2 μL of an LB overnight culture) adjacent to the *S.* Mg1. After incubation on thin agar plates (*SI Materials and Methods*), the agar layer was separated from the plates and used for MALDI imaging. Cultures were prepared for MALDI imaging by transferring the thin agar sections to a Bruker MSP 96 anchor plate. Universal Matrix was

deposited evenly over the agar by using a 53-μm test sieve. The agar with matrix was then dried in a 40 °C oven for 1–3 h until desiccated. The sample was dusted with a nitrogen stream and then inserted into a Microflex Bruker Daltonics mass spectrometer for data collection. The data were filtered manually by selecting ions of interest from the average spectrum or from individual spectra and is presented without normalization.

For IMS of wild type and Δ*sfhA S.* Mg1 activity, 1 μL of each spore stock (10^9 spores per mL; PSK0558 and PDS0366) were spotted 1.5 cm apart on a 10-mL GYM (2% agar) plate. Once dry, 3 μL of 23 mg/mL surfactin (69 μg) was placed on a filter disk between the inoculated spots. The plate was sealed with parafilm and incubated upside down at 30 °C for 48 h. Then, the sample was cut out of the plate and transferred to the MALDI target plate. The filter disk was removed, Universal Matrix was applied through a 53-μm sieve, and the sample was dehydrated at 37 °C. After the excess matrix was removed, IMS was performed in linear mode by using a Bruker Autoflex Speed at 600-μm resolution after calibrating to the Peptide Calibration Standard (Bruker 20619). Data were acquired from 500 to 1500 Da at 952 measurement points. The images were acquired by using a raster program as described (31). Extracted ion images were prepared by using TissueView 1.1 (AB SCIEX) and colored in Adobe Photoshop CS3.

Enzyme Activity Assays. Surfactin (50 μM, mixture of lipopeptides) and other antibiotics assayed (50 μM each) were reacted with purified hydrolase (320 ng) at ambient temperature in 100-μL assay buffer (50 mM Tris·HCl at pH 8.0, 150 mM NaCl, and 1 mM DTT). Reactions were quenched with 500 μL of acetone. Surfactin samples were quenched at time points of 0, 10, 20, 40, 60, and 120 min. A saturated solution of 20–30 mg/mL Universal Matrix dissolved in 1:1 acetonitrile:water with 0.2% TFA (1.0 μL) was cospotted on a MALDI plate with the quenched reaction mixture (1.0 μL), and MS1 spectra were collected on a Shimadzu Axima-CFR MALDI-TOF mass spectrometer. The extent of surfactin hydrolysis was determined (semi-quantitatively) by comparing the ratios of intact surfactin ion ($[M+Na]^+$) to hydrolyzed surfactin ion ($[M+Na+H_2O]^+$) for representative ions at the different time points.

ACKNOWLEDGMENTS. We thank Bill Russell and David Russell in the Texas A&M University (TAMU) Laboratory for Biological Mass Spectrometry within the Department of Chemistry; Larry Dangott, director of the Protein Chemistry Laboratory in the Department of Biochemistry and Biophysics; Xiangming Kong in the TAMU Biomolecular NMR Laboratory; Josh Blodgett at Harvard Medical School for providing the WM3780 *E. coli* for conjugation with *Streptomyces*; and Frank Raushel for critical reading of the manuscript. We thank Jared Silverman and Cubist Pharmaceuticals for supplying a sample of A54145D. We thank the Welch Foundation for Grant A-1796 and TAMU for funds to support this project. The IMS work was supported by National Institutes of Health Grant AI095125.

1. Chao L, Levin BR (1981) Structured habitats and the evolution of anticompetitor toxins in bacteria. *Proc Natl Acad Sci USA* 78:6324–6328.
2. Hibbing ME, Fuqua C, Parsek MR, Peterson SB (2010) Bacterial competition: Surviving and thriving in the microbial jungle. *Nat Rev Microbiol* 8:15–25.
3. Lina G, et al. (2003) Bacterial competition for human nasal cavity colonization: Role of Staphylococcal agr alleles. *Appl Environ Microbiol* 69:18–23.
4. Kirkup BC, Riley MA (2004) Antibiotic-mediated antagonism leads to a bacterial game of rock-paper-scissors in vivo. *Nature* 428:412–414.
5. Lemos ML, Dopazo CP, Toranzo AE, Barja JL (1991) Competitive dominance of antibiotic-producing marine bacteria in mixed cultures. *J Appl Bacteriol* 71:228–232.
6. Weaver VB, Kolter R (2004) Burkholderia spp. alter Pseudomonas aeruginosa physiology through iron sequestration. *J Bacteriol* 186:2376–2384.
7. Lenski RE, Hattingh SE (1986) Coexistence of two competitors on one resource and one inhibitor: A chemostat model based on bacteria and antibiotics. *J Theor Biol* 122:83–93.
8. Linares JF, Gustafsson I, Baquero F, Martinez JL (2006) Antibiotics as intermicrobial signaling agents instead of weapons. *Proc Natl Acad Sci USA* 103:19484–19489.
9. Wiener P (1996) Experimental studies on the ecological role of antibiotic production in bacteria. *Evol Ecol* 10:405–421.
10. D'Costa VM, McGrann KM, Hughes DW, Wright GD (2006) Sampling the antibiotic resistome. *Science* 311:374–377.
11. Sommer MO, Dantas G, Church GM (2009) Functional characterization of the antibiotic resistance reservoir in the human microflora. *Science* 325:1128–1131.
12. Wright GD (2010) Antibiotic resistance in the environment: A link to the clinic? *Curr Opin Microbiol* 13:589–594.
13. Wright GD (2011) Molecular mechanisms of antibiotic resistance. *Chem Commun (Camb)* 47:4055–4061.
14. Pascale G De, Wright GD (2010) Antibiotic resistance by enzyme inactivation: From mechanisms to solutions. *Chembiochem* 11:1325–1334.
15. Poole K (2004) Resistance to beta-lactam antibiotics. *Cell Mol Life Sci* 61:2200–2223.
16. Molina L, et al. (2003) Degradation of pathogen quorum-sensing molecules by soil bacteria: A preventive and curative biological control mechanism. *FEMS Microbiol Ecol* 45:71–81.
17. Dong YH, Xu JL, Li XZ, Zhang LH (2000) AiiA, an enzyme that inactivates the acylhomoserine lactone quorum-sensing signal and attenuates the virulence of Erwinia carotovora. *Proc Natl Acad Sci USA* 97:3526–3531.
18. Amara N, Krom BP, Kaufmann GF, Meijler MM (2011) Macromolecular inhibition of quorum sensing: Enzymes, antibodies, and beyond. *Chem Rev* 111:195–208.
19. Bernheimer AW, Avigad LS (1970) Nature and properties of a cytolytic agent produced by Bacillus subtilis. *J Gen Microbiol* 61:361–369.
20. Hashizume H, Nishimura Y (2008) Cyclic lipopeptide antibiotics. *Studies in Natural Products Chemistry* 35:693–751.
21. Peypoux F, Bonmatin JM, Wallach J (1999) Recent trends in the biochemistry of surfactin. *Appl Microbiol Biotechnol* 51:553–563.
22. Stein T (2005) Bacillus subtilis antibiotics: Structures, syntheses and specific functions. *Mol Microbiol* 56:845–857.
23. Bais HP, Fall R, Vivanco JM (2004) Biocontrol of Bacillus subtilis against infection of Arabidopsis roots by Pseudomonas syringae is facilitated by biofilm formation and surfactin production. *Plant Physiol* 134:307–319.
24. Kearns DB, Chu F, Rudner R, Losick R (2004) Genes governing swarming in Bacillus subtilis and evidence for a phase variation mechanism controlling surface motility. *Mol Microbiol* 52:357–369.
25. Kinsinger RF, Shirk MC, Fall R (2003) Rapid surface motility in Bacillus subtilis is dependent on extracellular surfactin and potassium ion. *J Bacteriol* 185:5627–5631.
26. López D, Fischbach MA, Chu F, Losick R, Kolter R (2009) Structurally diverse natural products that cause potassium leakage trigger multicellularity in Bacillus subtilis. *Proc Natl Acad Sci USA* 106:280–285.
27. Hofemeister J, et al. (2004) Genetic analysis of the biosynthesis of non-ribosomal peptide- and polyketide-like antibiotics, iron uptake and biofilm formation by Bacillus subtilis A1/3. *Mol Genet Genomics* 272:363–378.
28. Ongena M, et al. (2007) Surfactin and fengycin lipopeptides of Bacillus subtilis as elicitors of induced systemic resistance in plants. *Environ Microbiol* 9:1084–1090.
29. Vollenbroich D, Pauli G, Ozel M, Vater J (1997) Antimycoplasma properties and application in cell culture of surfactin, a lipopeptide antibiotic from Bacillus subtilis. *Appl Environ Microbiol* 63:44–49.
30. Straight PD, Willey JM, Kolter R (2006) Interactions between Streptomyces coelicolor and Bacillus subtilis: Role of surfactants in raising aerial structures. *J Bacteriol* 188: 4918–4925.
31. Yang Y-L, Xu Y, Straight P, Dorrestein PC (2009) Translating metabolic exchange with imaging mass spectrometry. *Nat Chem Biol* 5:885–887.
32. Lima TMS, et al. (2011) Biodegradability of bacterial surfactants. *Biodegradation* 22: 585–592.
33. Carrillo C, Teruel JA, Aranda FJ, Ortiz A (2003) Molecular mechanism of membrane permeabilization by the peptide antibiotic surfactin. *Biochimica et Biophysica Acta. Biomembranes* 1611:91–97.
34. Bonmatin JM, Genest M, Labbé H, Ptak M (1994) Solution three-dimensional structure of surfactin: A cyclic lipopeptide studied by 1H-NMR, distance geometry, and molecular dynamics. *Biopolymers* 34:975–986.
35. Kakinuma A, Sugino H, Isono M, Tamura G, Arima K (1969) Determination of fatty acid in surfactin and elucidation of the total structure of surfactin. *Agric Biol Chem* 33:973–976.
36. Thimon L, Peyoux F, Maget-Dana R, Michel G (1992) Surface-active properties of antifungal lipopeptides produced by Bacillus subtilis. *J Am Oil Chem Soc* 69:92–93.
37. Grangemard I, Wallach J, Peypoux F (1999) Evidence of surfactin hydrolysis by a bacterial endoprotease. *Biotechnol Lett* 21:241–244.
38. Watrous JD, Dorrestein PC (2011) Imaging mass spectrometry in microbiology. *Nat Rev Microbiol* 9:683–694.
39. Phelan VV, Liu W-T, Pogliano K, Dorrestein PC (2012) Microbial metabolic exchange–the chemotype-to-phenotype link. *Nat Chem Biol* 8:26–35.
40. Esquenazi E, et al. (2008) Visualizing the spatial distribution of secondary metabolites produced by marine cyanobacteria and sponges via MALDI-TOF imaging. *Mol Biosyst* 4:562–570.
41. Earl AM, Losick R, Kolter R (2007) Bacillus subtilis genome diversity. *J Bacteriol* 189: 1163–1170.
42. Hall BG (2004) Predicting the evolution of antibiotic resistance genes. *Nat Rev Microbiol* 2:430–435.
43. Walsh CT (2004) Polyketide and nonribosomal peptide antibiotics: Modularity and versatility. *Science* 303:1805–1810.
44. Kopp F, Marahiel MA (2007) Macrocyclization strategies in polyketide and nonribosomal peptide biosynthesis. *Nat Prod Rep* 24:735–749.
45. Butler MJ, et al. (1995) Cloning and characterization of a gene encoding a secreted tripeptidyl aminopeptidase from Streptomyces lividans 66. *Appl Environ Microbiol* 61: 3145–3150.
46. Debono M, et al. (1987) A21978C, a complex of new acidic peptide antibiotics: Isolation, chemistry, and mass spectral structure elucidation. *J Antibiot (Tokyo)* 40:761–777.
47. Gominet M, Seghezzi N, Mazodier P (2011) Acyl depsipeptide (ADEP) resistance in Streptomyces. *Microbiology* 157:2226–2234.
48. Kieser T, Bibb MJ, Buttner MJ, Chater KF, Hopwood DA (2000) *Practical Streptomyces Genetics* (John Innes Found, Norwich, UK).
49. Blodgett JAV, Zhang JK, Metcalf WW (2005) Molecular cloning, sequence analysis, and heterologous expression of the phosphinothricin tripeptide biosynthetic gene cluster from Streptomyces viridochromogenes DSM 40736. *Antimicrob Agents Chemother* 49:230–240.